PERGAMON

PII: S1359-6454(99)00026-9

Acta mater. Vol. 47, No. 5, pp. 1627–1634, 1999

Printed in Great Britain
1359-6454/99 $20.00 + 0.00

EXPERIMENTAL INVESTIGATION AND MODELING OF THE INFLUENCE OF MICROSTRUCTURE ON THE RESISTIVE CONDUCTIVITY OF A Cu–Ag–Nb *IN SITU* COMPOSITE

D. MATTISSEN[1], D. RAABE†[1]‡ and F. HERINGHAUS[2]

[1]Institut für Metallkunde und Metallphysik, RWTH Aachen, 52056 Aachen, Germany and [2]Degussa AG, Edelmetall Forschung und Entwicklung, 63457 Hanau, Germany

(Received 18 May 1998; accepted 21 December 1998)

Abstract—A Cu–8.2 wt% Ag–4 wt% Nb *in situ* metal matrix composite was manufactured by inductive melting, casting, swaging, and wire drawing. The final wire ($\eta = \ln(A_0/A) = 10.5$, A: wire cross section) had a strength of 1840 MPa and 46% of the conductivity of pure Cu. The electrical resistivity of the composite wires was experimentally investigated as a function of wire strain and temperature. The microstructure was examined by means of optical and electron microscopy. The observed decrease in conductivity with increasing wire strain is interpreted in terms of inelastic electron scattering at internal phase boundaries. The experimental data are in very good accord with the predictions of an analytical size-effect model which takes into account the development of the filament spacing as a function of wire strain and the mean free path of the conduction electrons as a function of temperature. The experimentally obtained and calculated resistivity data are compared to those of the pure constituents. © *1999 Acta Metallurgica Inc. Published by Elsevier Science Ltd. All rights reserved.*

1. INTRODUCTION

Due to their combination of high strength and good electrical conductivity, *in situ* processed Cu-based metal matrix composites (MMCs) are considered as candidate materials for the production of highly mechanically stressed electrical devices. Applications in the fields of steady state and long-pulse high-field resistive magnet design [1–7] and industrial robotics [8] are of particular interest in this context.

Most studies in the past concentrated on the investigation of binary Cu–Nb [9–20] and Cu–Ag composites [21–26]. Copper and niobium form a quasi monotectic system and have no mutual solubility by practical means [27, 28]. During casting the Nb solidifies dendritically and forms into thin elongated curled filaments during wire drawing. Alloys consisting of Cu and 20 wt% Nb have an ultimate tensile strength (UTS) of up to 2.2 GPa ($\eta = 12$) [12, 13, 16, 17].

Copper and silver form a simple eutectic system with limited substitutional solubility [29]. Alloys containing more than 6 wt% Ag usually reveal two phases, a Cu-rich solid solution and a Cu–Ag eutectic. During deformation the eutectic and the Cu-rich matrix form into lamellar filaments. An intermediate heat treatment leads to Ag precipitations. These can be used to increase the matrix strain and to form additional fibers during further drawing. After large wire strains Cu–Ag MMCs reveal an UTS of up to $\sigma = 1.5$ GPa ($\eta = 10$) [22, 23].

In continuation of these studies on binary alloys recent work focused on the development of a new generation of ternary *in situ* Cu–Ag–Nb composites with the aim to combine the hardening effects of both Nb and Ag [30–34].

While the processing and the mechanical properties of these ternary compounds have been the subject of previous publications [30–34], their electromagnetic properties have not yet been studied. The electrical conductivity of heavily deformed Cu- or Ag-based composites is typically smaller than expected from the linear rule of mixtures (ROM). This effect is commonly referred to as size effect. It is due to inelastic scattering of the conduction electrons at the internal phase boundaries [9, 20, 26, 35, 36].

This study presents an experimental investigation of the evolution of the resistive electrical conductivity of a heavily wire drawn ternary Cu–8.2 wt% Ag–4 wt% Nb *in situ* processed MMC as a function of wire strain and temperature and its dependence on the microstructure. The experimental observations are quantitatively compared to predictions of an analytical size-effect model which takes into account the development of the filament spacing as a function of the wire strain.

†Present address: Luchweg 10, 14621 Schönwalde, Germany.

‡To whom all correspondence should be addressed.

2. SAMPLE PREPARATION

A Cu–8.2 wt% Ag–4 wt% Nb alloy was prepared by inductive melting using a frequency of 10 kHz and a power of 50 kW [33]. All constituents had an initial purity of at least 99.995%. Ingots of 18 mm diameter were cast under an argon atmosphere at a pressure of 0.6×10^5 Pa. A crucible and a mould of high purity graphite were used. The mould was preheated to about 600°C to ensure good fluidity and filling. From the cast cylindrical ingots wires were produced by rotary swaging and drawing through hard metal drawing bench dies. A maximum true wire strain above $\eta = 10$ ($\eta = \ln(A_0/A)$, A: wire cross section) was attained without intermediate annealing. Further processing details are reported elsewhere [33, 37].

3. EXPERIMENTAL PROCEDURE

3.1. Experimental investigation of the microstructure

Optical and scanning electron microscopy (SEM) were used to determine the morphology and topology both of the Cu matrix and of the Ag and Nb filaments. Due to insufficient contrast, an unambiguous optical identification of the various phases was sometimes not possible. The samples were thus additionally analyzed using energy-disperse X-ray spectrometry (EDX). The morphology of the isolated Nb fibers was also investigated by use of a selective etching technique, where the Cu and Ag were dissolved by dilute nitric acid. Details about the experimental procedure were reported previously [32].

3.2. Experimental investigation of the resistive electrical conductivity

Systematic measurements of the resistive conductivity at 298 and 77 K as a function of the wire strain were carried out for Cu–8.2 wt% Ag–4 wt% Nb by means of the direct current (d.c.) four-probe technique using a sample current of 100 mA. For a number of Cu–8.2 wt% Ag–4 wt% Nb, pure Cu, pure Ag, and pure Nb wires of identical total wire strain; the influence of the temperature on the resistive conductivity was studied within the temperature range 3–350 K.

4. EXPERIMENTAL RESULTS

4.1. Microstructure evolution as a function of wire strain

Figure 1 shows the development of the diameters of the Cu matrix phase (d_{Cu}), the Nb filaments (d_{Nb}), and the Ag filaments (d_{Ag}) in the composite

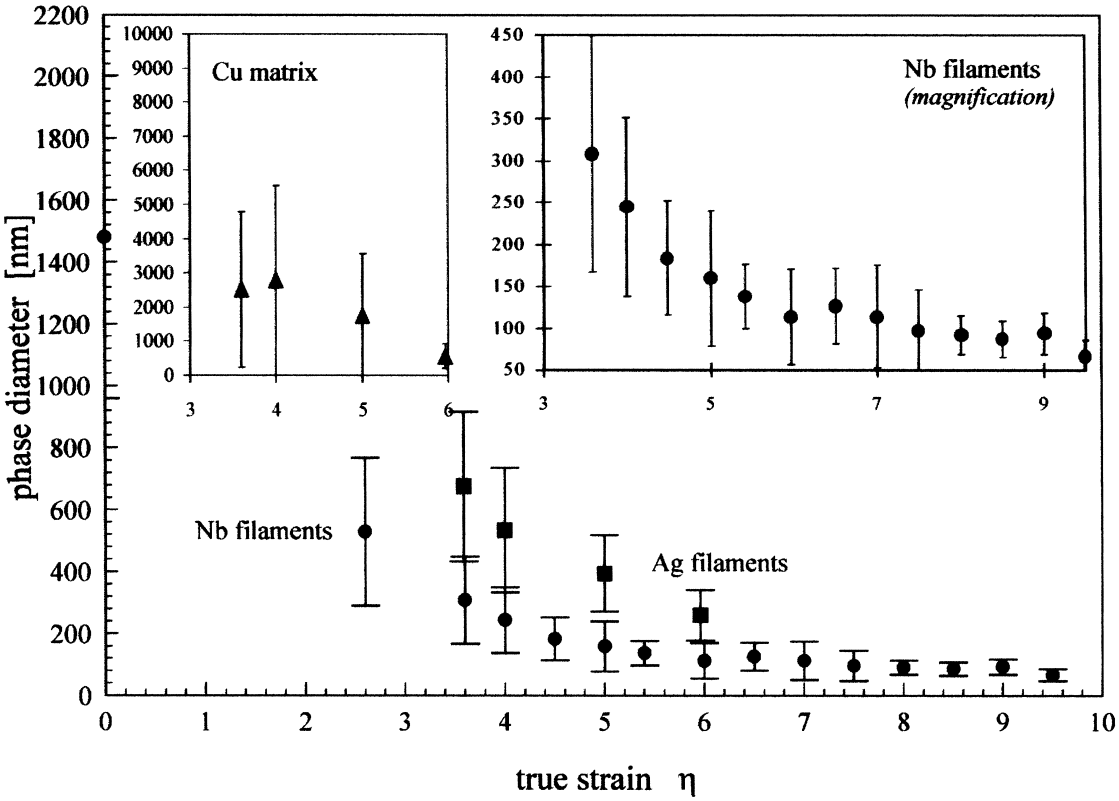

Fig. 1. Development of the diameters of the Nb filaments, the Ag filaments, and the Cu matrix phase in the Cu–8.2 wt% Ag–4 wt% Nb composite as investigated by quantitative SEM.

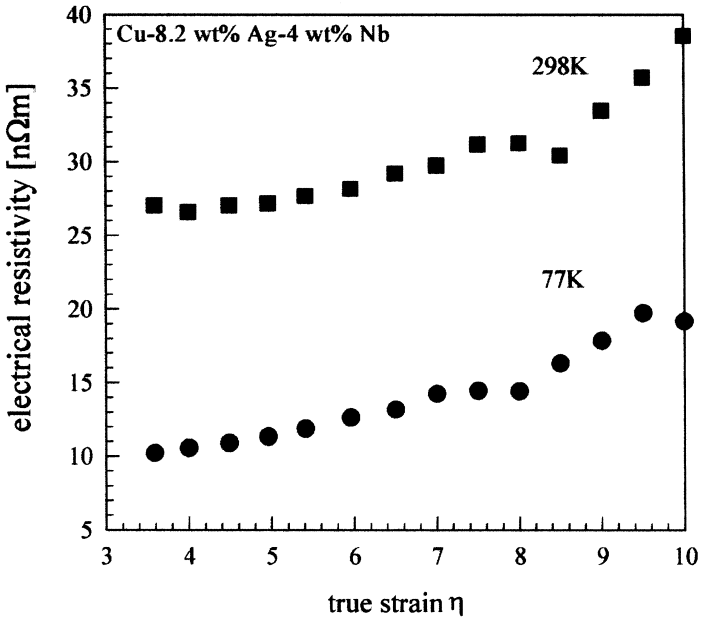

Fig. 2. Electrical resistivity of the ternary Cu–8.2 wt% Ag–4 wt% Nb composite as a function of the true (logarithmic) wire strain η ($\eta = \ln(A_0/A)$, A: wire cross section) at $T = 298$ and 77 K.

as a function of the true wire strain η. At low strains the Ag filaments were thicker and shorter than the Nb filaments. With increasing strain their average thickness became more similar to that of the Nb filaments. At a wire strain of $\eta = 3.6$ the average Ag filament diameter amounted to $d_{Ag} \approx 676$ nm and at $\eta = 6$ to $d_{Ag} \approx 260$ nm. At a wire strain of $\eta = 2.6$ the average Nb filament diameter amounted to $d_{Nb} \approx 529$ nm and at $\eta = 9.5$ to $d_{Nb} \approx 66$ nm.

For including the evolution of the filament morphology in an analytical size-effect model the average phase diameters were exponentially fitted from the metallographic data according to $d_{Cu} = 31767\ \text{nm} \times \exp(-0.6415\,\eta)$, $d_{Ag} = 2630\ \text{nm} \times \exp(-0.3861\,\eta)$, and $d_{Nb} = 1386.6\ \text{nm} \times \exp(-0.413\,\eta)$.

4.2. Resistive conductivity as a function of wire strain and temperature

Figure 2 shows the dependence of the electrical resistivity of Cu–8.2 wt% Ag–4 wt% Nb on the strain at 298 and 77 K. At true wire strains above $\eta = 8.5$ the conductivity decreases drastically. The increase in the resistivity with increasing strain is more pronounced at 77 K (from $\sim$10 nΩ m at $\eta =$ 3.5 to $\sim$20 nΩ m at $\eta \approx 10$) than at 298 K (from $\sim$27 nΩ m at $\eta = 3.5$ to $\sim$38 nΩ m at $\eta \approx 10$). Consequently, the resistivity ratio of Cu–8.2 wt% Ag–4 wt% Nb, $\rho(298\ \text{K})/\rho(77\ \text{K})$, drops as a function of the true wire strain (Fig. 3).

At temperatures below the transition temperature of pure Nb the wire drawn Cu–8.2 wt% Ag–4 wt%

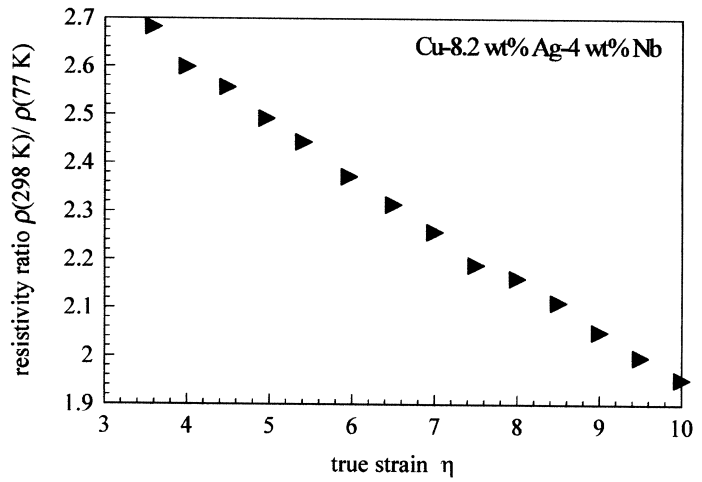

Fig. 3. Electrical resistivity ratio $\rho(298\ \text{K})/\rho(77\ \text{K})$ of the ternary Cu–8.2 wt% Ag–4 wt% Nb composite as a function of the true (logarithmic) wire strain η ($\eta = \ln(A_0/A)$, A: wire cross section).

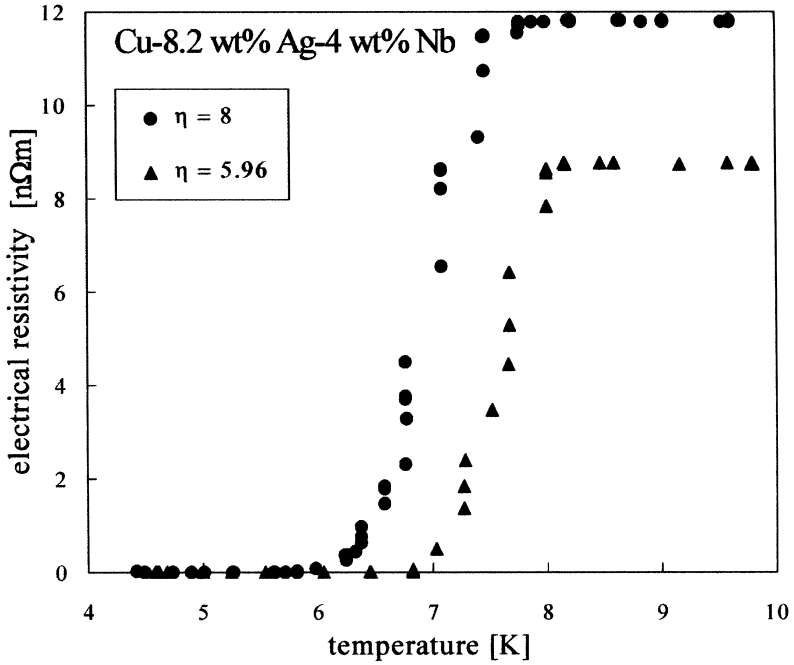

Fig. 4. Transition of the electrical resistivity of the ternary Cu–8.2 wt% Ag–4 wt% Nb composite from the normal resistive state to the superconducting state as a function of temperature for two different degrees of the true (logarithmic) wire strain ($\eta = 8$, $\eta = 5.96$) ($\eta = \ln(A_0/A)$, A: wire cross section).

Nb reveals superconducting properties. Figure 4 shows for the composite the transition to the superconducting state as a function of strain. The data reveal that an increasing wire strain leads to a shift of the transition temperature to lower values. A detailed analysis of the superconducting properties of the ternary composite is given in Ref. [38] based on Ginzburg–Landau theory.

The electrical resistivity of pure Cu wires and pure Ag wires was practically independent of the degree of deformation and was always lower than for the composite (Fig. 5). The effect of deformation on the resistivity temperature coefficient of pure Cu, pure Ag, pure Nb, and Cu–8.2 wt% Ag–4 wt% Nb is given in Fig. 6. While the temperature coefficient of the pure wires is practically independent on wire strain, that of the composite drops with increasing wire strain.

5. MODELING OF THE ELECTRICAL RESISTIVITY OF THE Cu–Ag–Nb COMPOSITE

5.1. Fundamentals of the model

Any analytical calculation of absolute values of the electrical resistivity of MMCs requires very detailed data both on the impurity content and distribution and on the density and distribution of the lattice defects (e.g. dislocation density, grain size, etc.). Since these data are usually not known with sufficient reliablility, analytical models of the resistivity of composites are commonly exclusively based on the size effect, which typically provides by far the most dominant contribution to inelastic internal scattering of the conduction electrons in such materials [9, 20, 26, 35, 36]. The predictions of such models can then be compared to the relative changes observed experimentally.

Analytical predictions of the electrical resistivity of composites on the basis of the size effect require the volume fractions and the topologies of each phase in the composite and some intrinsic constants.

The model starts with the calculation of the electrical resistivity of each phase according to the phenomenological expression for surface and phase boundary scattering given by Sondheimer [39]

$$\rho(d) = \rho_0\left(1 + \frac{3}{4}(1-p)\frac{l_0(T)}{d}\right) \qquad (1)$$

where $\rho(d)$ is the resistivity as a function of the filament thickness, ρ_0 the resistivity for a sample without scattering at phase boundaries (infinite sample or phase size), p the scattering factor, l_0 the mean free path of the conduction electrons in that particular phase and d the thickness of the filament. According to Dingle [35] the scattering factor p represents the probability of elastic scattering and $(1-p)$ that of inelastic scattering at the phase boundary.

The mean free paths of the conduction electrons in the various phases (as a function of temperature) were determined from the temperature dependent resistivities of the bulk phases using

$$\sigma(T)l_0(T) = \frac{e^2 N_{\mathrm{el}}}{\hbar V}\left(3\pi^2 \frac{N_{\mathrm{el}}}{V}\right)^{-1/3} \qquad (2)$$

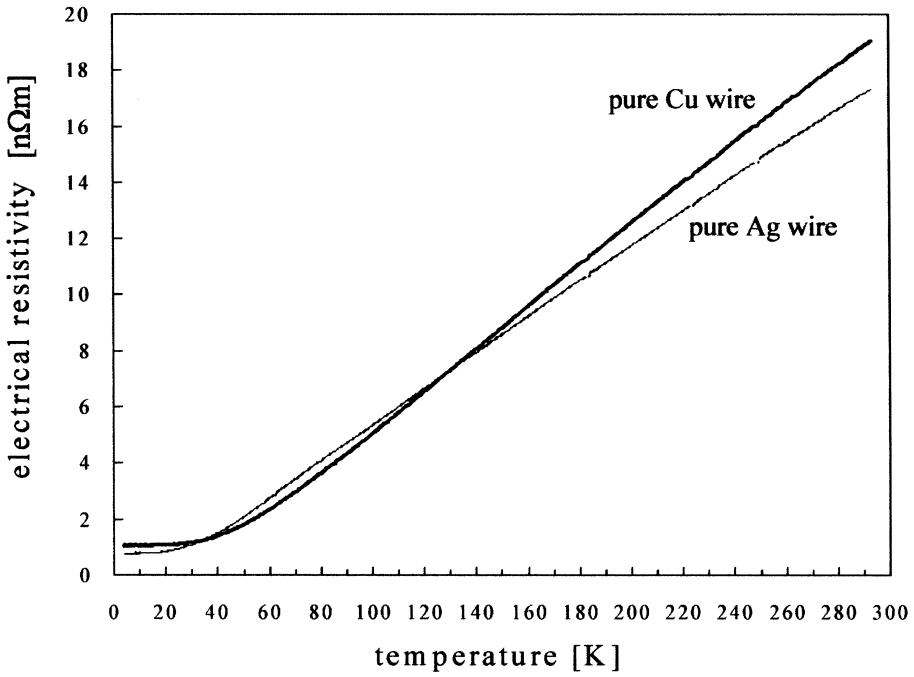

Fig. 5. Electrical resistivity of pure Cu and pure Ag as a function of temperature.

where $\sigma(T)$ is the conductivity and N_{el}/V the electron density. The right-hand side of equation (2) was calculated using a value of $N_{el}/V = 5.57 \times 10^{29}/m^3$ under the assumption of monovalence for Ag and Cu and a value of $N_{el}/V = 5.325 \times 10^{29}/m^3$ for Nb.

Finally, the individual resistivities ρ_i of the phases were topologically combined to give the overall resistivity of the composite ρ_{MMC}. The model treats all phases as resistors that are arranged parallel

$$\rho_{MMC} = \left(\sum_{i=1}^{n} \frac{f_i}{\rho_i}\right)^{-1} \tag{3}$$

where the f_i are the volume fractions of the phases $i = 1, \ldots, n$, and ρ_i the electrical resistivities of the phases $i = 1, \ldots, n$.

5.2. *Application of the model*

The prediction of the electrical resistivity of the Cu–8.2 wt% Ag–4 wt% Nb composite on the basis of equations (1)–(3) requires some topological con-

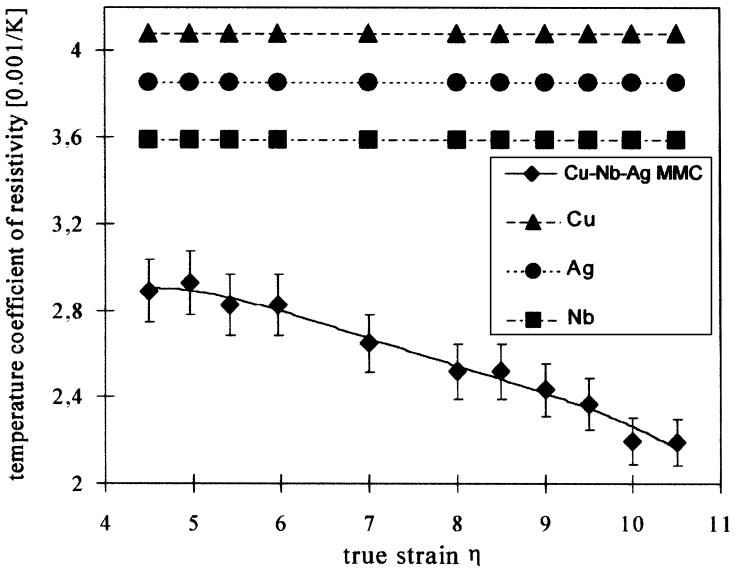

Fig. 6. Temperature coefficient of the electrical resistivity of Cu, Ag, Nb, and the ternary Cu–8.2 wt% Ag–4 wt% Nb composite between 273 and 373 K as a function of the true (logarithmic) wire strain η ($\eta = \ln(A_0/A)$, A: wire cross section).

siderations about the incorporation of the topology of the Ag filaments. In the as-cast sample the Ag had a lamellar shape and formed a Ag–Cu eutectic whilst the Nb was precipitated in the form of isolated Wulff polyhedra and dendrites [32, 33]. Therefore, the composite was treated as a material consisting of two primary phases, namely, 95.82 vol.% Cu–Ag and 4.18 vol.% Nb, in which the former consists of two sub-phases, namely, 91.92 vol.% Cu and 8.08 vol.% Ag. The weight fractions of the primary phases and of the sub-phases were calculated from the weight composition of Cu–8.2 wt% Ag–4 wt% Nb as (90.66 wt% Cu–9.34 wt% Ag)–4 wt% Nb and the volume fractions correspondingly as (91.92 vol.% Cu–8.08 vol.% Ag)–4.18 vol.% Nb. Equation (3) was first applied to the two sub-phases Cu and Ag which then in turn were combined parallel with Nb to form the overall composite.

Values for the interface scattering factors p associated with the Cu–Ag interfaces were taken from previous investigations and simulations on this binary system [27]. These were for Cu–Ag: $p = 0.81$ at $T = 298$ K and $p = 0.84$ at $T = 77$ K. The size-effect approach as outlined in equation (1) can be derived from the Boltzmann transport equation for cases where $d > l_0$. This condition holds for the Cu ($d_{Cu}/l_{0\,Cu} \approx 3$), the Ag ($d_{Ag}/l_{0\,Ag} \approx 3$), and the Nb phase ($d_{Nb}/l_{0\,Nb} \approx 20$) corresponding to the current data for $\eta = 10$ and $T = 293$ K.

5.3. *Predictions of the model*

The predictions of the size-effect model for the composite, Cu–8.2 wt% Ag–4 wt% Nb, and for the various phases, Cu, Ag, Cu–Ag, and Nb, are given in Fig. 7 as a function of the wire strain at $T =$ 77 K [Fig. 7(a) and (b)] and at $T = 298$ K [Fig. 7(c) and (d)]. A strong effect can be found in the Cu and Ag phases and thus also in Cu–Ag, whereas Nb reveals only weak changes with deformation. Figure 7(b) ($T = 77$ K) and (d) ($T = 298$ K) show that a very good agreement between the model and the experimental data is found at low and elevated strains, particularly for $T = 298$ K, while the model slightly underpredicts the resistivity at intermediate strains between $\eta = 6$ and 8.

6. DISCUSSION

The resistivity of Cu–8.2 wt% Ag–4 wt% Nb increases considerably with the degree of deformation. The strong dependence may be chiefly attributed to the scattering of conduction electrons at the various internal phase boundaries. This effect becomes particularly pronounced when the average filament spacing is, after heavy deformation, of the same order of magnitude as the mean free path of the conduction electrons in the Cu and the Ag phase (Figs 2 and 7) [9, 36]. Since the mean free electron path linearly decreases as a function of temperature in the regime above the Debye temperature, due to the increase of phonon scattering, the contribution of interface scattering to the overall resistivity is more pronounced at low temperatures [Fig. 7(b), increase by ~100%] than at elevated temperatures [Fig. 7(d), increase by ~40%]. Since the Cu–Ag interfaces have a low, and the Cu–Nb and Ag–Nb interfaces a very high effect on inelastic scattering, the latter are assumed to be primarily responsible for the observed increase in resistivity.

The density of deformation induced lattice dislocations is of minor importance for the dependence of the resistivity on wire strain since only their cores add to the electrical resistivity, but contribute only a very small resistivity change per unit length of a dislocation [36, 40, 41]. Here the applied d.c. four-probe technique is not accurate enough to exactly account for such a change.

The composite (Cu–8.08 vol.% Ag)–4.18 vol.% Nb can be described as consisting of two first-order phases, 95.82 vol.% Cu–Ag and 4.18 vol.% Nb, the former of which consists of two second-order phases, 91.8 vol.% Cu and 8.08 vol.% Ag (see Fig. 7). Using this approach enables one to make an analytical topological prediction of the size effect due to interface scattering. A determination of the absolute values of the electrical resistivity is not feasible due to the effects of impurities and mutual solution. The latter, although of particular importance in the Cu–Ag phase, cannot be incorporated owing to the unavailability of appropriate experimental data.

In this context the slight discrepancy found at intermediate degrees of deformation between model and experiment [see Fig. 7(b) and (d)] may be qualitatively attributed to deformation-induced changes in the solubility or in the state of precipitation. While changes in the solubility can be explained in terms of the Gibbs–Thomson equation, which relates solubility to interface curvature, changes in the precipitation state can only be attributed to frictional heating of the sample during wire drawing.

However, both effects may either not be as dominant anymore at high degrees of deformation [i.e. at strain above $\eta = 8$, see Fig. 7(b) and (d)] due to the dominance of strong interface scattering, or be reverted owing to the presence of a high density of internal interfaces. The latter argument, however, is not covered by experimental evidence and thus is of speculative character.

Regarding the effect of the microstructure of the individual phases on inelastic scattering [Fig. 7(a) and (c)], it may be concluded that the size effects in the Cu phase and in the Ag phase are chiefly responsible for the observed increase in the electrical resistivity of the Cu–Ag phase and thus ultimately of the ternary composite. In comparison to the Cu phase and the Cu–Ag phase, the size effect in Ag, particularly at large strains, is much stronger at

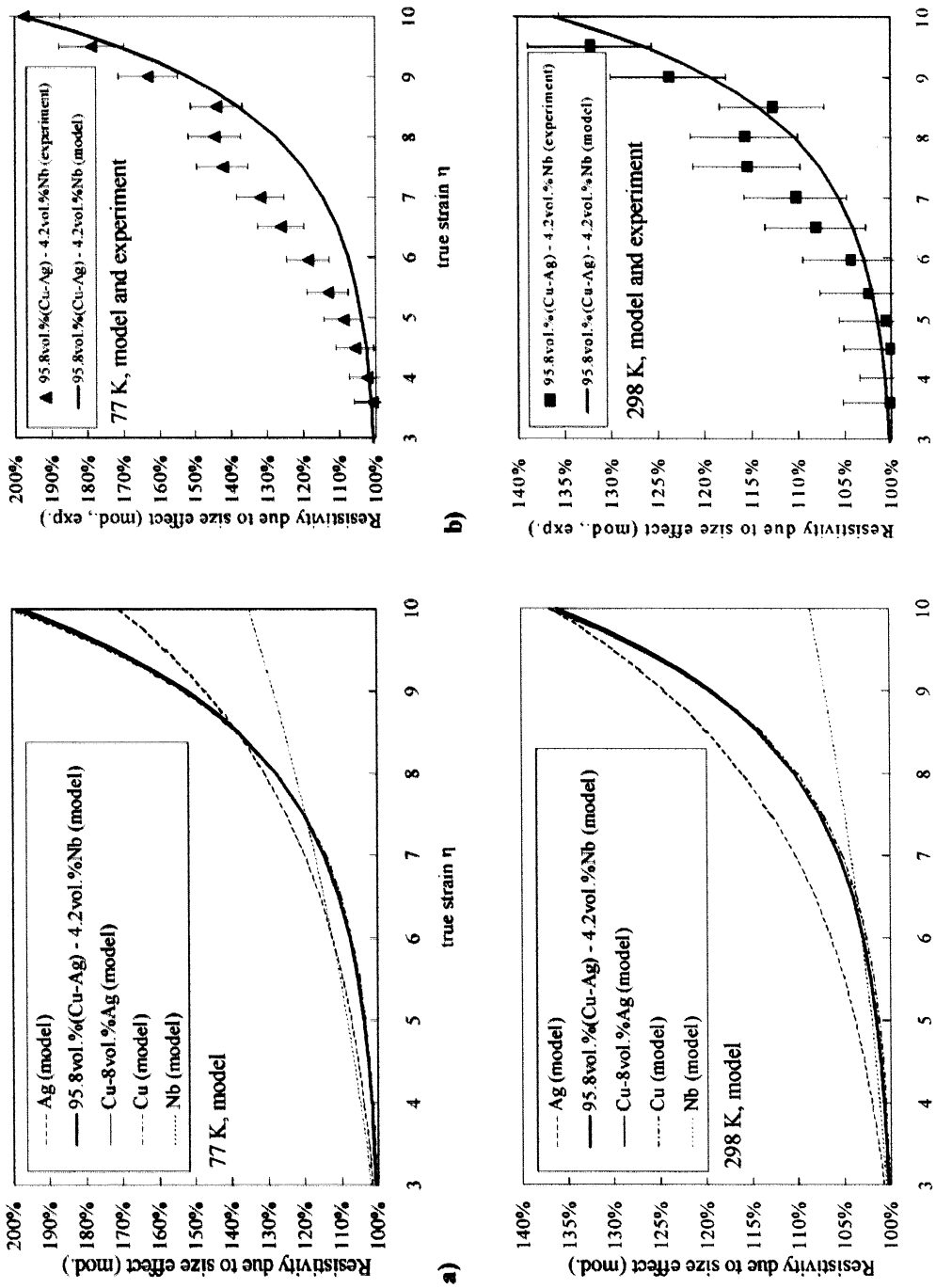

Fig. 7. Modeled and experimentally observed relative changes of the electrical resistivity of Cu, Nb, Ag, and the ternary Cu–8.2 wt% Ag–4 wt% Nb composite at $T = 298$ and 77 K as a function of the true (logarithmic) wire strain η ($\eta = \ln(A_0/A)$, A: wire cross section). (a) $T = 77$ K, size effect model for the various phases and for the composite. (b) $T = 77$ K, comparison between size-effect model and experimental data. (c) $T = 298$ K, size-effect model for the various phases and for the composite. (d) $T = 298$ K, comparison between size-effect model and experimental data.

$T = 298$ K [Fig. 7(a)] than at $T = 77$ K [Fig. 7(c)]. This effect is due to the stronger temperature-dependence of the mean free electron path in Cu as compared to Ag.

7. CONCLUSIONS

A ternary *in situ* Cu–8.2 wt% Ag–4 wt% Nb MMC was manufactured by melting, casting, swaging, and wire drawing. The microstructure was investigated using electron microscopy and EDX. The resistive conductiving properties were examined using four-probe d.c. tests at various temperatures. The main results are:

- The ternary MMC was very ductile. A maximum wire strain of $\eta = 10.5$ was reached without intermediate annealing.
- Wires of the ternary MMC of maximum strain ($\eta_{max} = 10.5$) had an UTS of 1840 MPa and 46% of the conductivity of pure Cu (IACS).
- The electrical resistivity of the ternary MMC at large strains drastically increased with increasing strain. This was attributed to the size effect, i.e. to the inelastic scattering of the conduction electrons at the internal interfaces.
- The influence of the size effect on the course of the electrical resistivity of the ternary MMC was modeled using an analytical solution of the Boltzmann transport equation. At low and very large strains the model was in very good accord with the experimental data. At intermediate strains between $\eta = 6$ and 8 the model underpredicted the resistivity. This deviation was interpreted in terms of changes in the solubility and probably in the precipitation state.

Acknowledgements—The authors are indebted to G. Gottstein, H.-J. Scheider-Muntau, and J.D. Embury for helpful discussions. One of the authors (D.R.) gratefully acknowledges the financial support by the Deutsche Forschungsgemeinschaft through the Heisenberg program and by the National High Magnetic Field Laboratory in Tallahassee, Florida.

REFERENCES

1. Foner, S. and Bobrov, E., *I.E.E.E. Magn.*, 1987, **24**, 1059.
2. Asano, T., Sakai, Y., Inoue, K., Oshikiri, M. and Maeda, H., *I.E.E.E. Magn.*, 1992, **28**, 888.
3. Heringhaus, F., Eyssa, Y. M., Pernambuco-Wise, P., Bird, M. D., Gottstein, G. and Schneider-Muntau, H.-J., *Metall.*, 1996, **50**, 272.
4. Embury, J. D., Hill, M. A., Spitzig, W. A. and Sakai, Y., *MRS Bull.*, 1993, **8**, 57.
5. Heringhaus, F., Leffers, R., Gottstein, G. and Schneider-Muntau, H.-J., *Processing, Properties, and Application of Cast Metal Matrix Composites, TMS Fall Meeting*, Vol. 1, 1996, p. 127.
6. Schneider-Muntau, H.-J., *I.E.E.E. Trans. Magn.*, 1982, **18**, 32.
7. Wood, J. T., Embury, J. D. and Ashby, M. F., *Acta mater.*, 1997, **45**, 1099.
8. Raabe, D., Matissen, K., Miyake, K., Takahara, H. and Heringhans, F., in *Proc. Int. Conf. "Dialogues at Lake Louise" 1997, Composites—Design for Performance*, ed. P. S. Nicholson. Eagle Press, Burington, Ontario, Canada, pp. 146–154.
9. Bevk, J., Harbison, J. P. and Bell, J. L., *J. appl. Phys.*, 1978, **49**, 6031.
10. Karasek, K. R. and Bevk, J., *J. appl. Phys.*, 1981, **52**, 1370.
11. Funkenbusch, P. D. and Courtney, T. H., *Acta metall.*, 1985, **33**, 913.
12. Spitzig, W. A., Pelton, A. R. and Laabs, F. C., *Acta metall.*, 1987, **35**, 2427.
13. Funkenbusch, P. D., Lee, J. K. and Courtney, T. H., *Metall. Trans. A*, 1987, **18**, 1249.
14. Chumbley, L. S., Downing, H. L., Spitzig, W. A. and Verhoeven, J. D., *Mater. Sci. Engng*, 1989, **A117**, 59.
15. Hong, S. I., Hill, M. A. and Embury, J. D., *Acta metall.*, 1995, **43**, 3313.
16. Spitzig, W. A., *Acta metall.*, 1991, **39**, 1085.
17. Spitzig, W. A., Downing, H. L., Laabs, F. C., Gibson, E. D. and Verhoeven, J. D., *Metall. Trans. A*, 1993, **24**, 7.
18. Hangen, U. and Raabe, D., *Acta metall.*, 1995, **43**, 4075.
19. Heringhaus, F., Raabe, D. and Gottstein, G., *Acta metall.*, 1995, **43**, 1467.
20. Raabe, D., Heringhaus, F., Hangen, U. and Gottstein, G., *Z. Metallk.*, 1995, **86**, 405.
21. Cline, H. E. and Lee, D., *Acta metall.*, 1970, **18**, 315.
22. Frommeyer, G. and Wassermann, G., *Physica status solidi (a)*, 1975, **27**, 99.
23. Frommeyer, G. and Wassermann, G., *Acta metall.*, 1975, **23**, 1353.
24. Sakai, Y., Inoue, K. and Maeda, H., *Acta metall.*, 1995, **43**, 1517.
25. Sakai, Y. and Schneider-Muntau, H.-J., *Acta mater.*, 1997, **45**, 1017.
26. Heringhaus, F., Ph.D. thesis, Institut für Metallkunde und Metallphysik, RWTH Aachen, Germany and National High Magnetic Field Laboratory, Tallahassee, U.S.A., 1998.
27. Sohn, K. Y., Ph.D. thesis, Department for Materials Science and Engineering, University of Florida, Gainesville, U.S.A., 1997.
28. Chakrabati, D. J. and Laughlin, D. E., *Bull. Alloy Phase Diagrams*, 1982, **2**, 936.
29. Terekhov, G. I. and Aleksandrova, L. N., *Izv. Akad. Nauk SSR. Metally*, 1984, **4**, 210.
30. Murray, J. L., *Metall. Trans. A*, 1984, **15**, 261.
31. Spitzig, W. A., Unpublished data.
32. Raabe, D. and Mattissen, D., *Acta mater.*, 1998, **46**, 5973.
33. Raabe, D. and Mattissen, D., *Metall.*, 1997, **51**, 464.
34. Raabe, D., Mattissen, D., Miyake, K., Takahara, H. and Heringhaus, F., in: *Proceedings of an International Conference "Dialogues at Lake Louise, Composites—Design for Performance"*, ed. P. S. Nicholson. Eagle Press, Burlington, Ontario, Canada, 1997, p. 146.
35. Dingle, R. B., *Proc. Soc. Lond. Ser.*, 1950, **201**, 545.
36. Raabe, D., *Comput. Mater. Sci.*, 1995, **3**, 402.
37. Mattissen, D., Diplomarbeit, Institut für Metallkunde und Metallphysik, RWTH Aachen, Germany, 1997.
38. Raabe, D. and Mattissen, D., *Acta mater.*, 1999, **47**, 769.
39. Sondheimer, E. H., *Adv. Phys.*, 1952, **1**, 1.
40. Blewit, T. H., Coltmann, R. R. and Rebstock, J. K., *Phil. Mag.*, 1957, **2**, 323.
41. Buck, O., *Physica status solidi*, 1962, **2**, 535.